THE UNIVERSITY of EDINBURGH

Edinburgh Research Explorer

Time-zoomable FRET Spectroscopy with a 512 x16 SPAD Line Sensor

Citation for published version:
Erdogan, A, Williams, G, Usai, A, Krstajic, N, Finlayson, N, beavil, A, Beavil, R & Henderson, R 2018, Time-zoomable FRET Spectroscopy with a 512 x16 SPAD Line Sensor. in *PROCEEDINGS VOLUME 10504 Biophysics, Biology and Biophotonics III: the Crossroads.* vol. 10504, 105040M, SPIE, Photonics West 2018, San Franisco, United States, 27/01/18. https://doi.org/10.1117/12.2290058

Digital Object Identifier (DOI):
10.1117/12.2290058

Link:
Link to publication record in Edinburgh Research Explorer

Published In:
PROCEEDINGS VOLUME 10504 Biophysics, Biology and Biophotonics III

General rights
Copyright for the publications made accessible via the Edinburgh Research Explorer is retained by the author(s) and / or other copyright owners and it is a condition of accessing these publications that users recognise and abide by the legal requirements associated with these rights.

Take down policy
The University of Edinburgh has made every reasonable effort to ensure that Edinburgh Research Explorer content complies with UK legislation. If you believe that the public display of this file breaches copyright please contact openaccess@ed.ac.uk providing details, and we will remove access to the work immediately and investigate your claim.

Download date: 01. Dec. 2022

Time-zoomable FRET Spectroscopy with a 512 x16 SPAD Line Sensor

Ahmet T. Erdogan[a], Gareth O.S. Williams[b], Andrea Usai[a], Nikola Krstajic[a,b], Neil Finlayson[a], Andrew Beavil[c], Rebecca Beavil[c] Robert K. Henderson[a]

[a]School of Engineering, Institute for Integrated Micro and Nano Systems, University of Edinburgh, King's Buildings, Alexander Crum Brown Road, Edinburgh EH 9 3FF, UK
[b]EPSRC IRC Hub in Optical Molecular Sensing & Imaging, Centre for Inflammation Research, Queen's Medical Research Institute, University of Edinburgh, 47 Little France Crescent, Edinburgh EH16 4TJ, UK
[c]Randall Division of Cell and Molecular Biophysics, King's College London, London, SE1 1UL, UK

ABSTRACT

We demonstrate a new 512x16 single photon avalanche diode (SPAD) based line sensor with per-pixel TCSPC histogramming for time-resolved, time-zoomable, FRET spectroscopy. The line sensor can operate in single photon counting (SPC) mode as well as time-correlated single photon counting (TCSPC) and per-pixel histogramming modes. TCSPC has been the preferred method for fluorescence lifetime measurements due to its collection of full decays as a histogram of arrival times. However, TCSPC is slow due to only capturing one photon per exposure and large timestamp data transfer requirements for offline histogramming. On-chip histogramming improves the data rate by allowing multiple SPAD pulses (up to one pulse per laser period) to be processed in each exposure cycle, along with secondly reducing the I/O bottleneck as only the final histogram is transferred. This can enable 50x higher acquisition rates (up to 10 billion counts per second), along with time-zoomable histogramming operation from 1.6ns to 205ns with 50ps resolution. A broad spectral range can be interrogated with the sensor (450-900nm). Overall, these sensors provide a unique combination of light sensing capabilities for use in high speed, sensitive, optical instrumentation in the time/wavelength domain. We test the sensor performance by observation of fluorescence resonance energy transfer (FRET) between FAM and TAMRA and between EGFP and RFP FRET standards.

Keywords: SPAD, Single Photon Counting, TCSPC, Histogram, Spectroscopy, Fluorescence lifetime, FRET, CMOS.

1. INTRODUCTION

A key aspect of time-resolved fluorescence is the decay constant (fluorescence lifetime) characterising the average time needed for a fluorophore molecule to go from the excited to ground state.[1] Changes in the environment surrounding the fluorophore (including the presence of other nearby fluorophores) can trigger changes in the fluorescence lifetime. Förster resonance energy transfer (FRET) involves the interaction of two molecules with overlapping energy levels in close proximity and is of increasing importance in studying protein-protein interactions. Applications range from molecular imaging, study of endogenous fluorescence lifetime in tissues, and analytical chemistry. FRET sensors are used to study the structure, conformation, hybridization and auto sequencing of nucleic acids[2] and to support diagnosis of common diseases such as cancer or Alzheimer's through analysis of lifetime changes arising from changes in pH inside cells.

Time-correlated single-photon counting (TCSPC) is a well-established technique for measuring fluorescence lifetimes.[3] Time-correlated single-photon counting spectroscopy enables the measurement of photon arrival times and numbers as a function of wavelength, with rich applications in nanosecond-scale fluorescence lifetime microscopy, Raman, FRET and bio-medical confocal imaging of cells. TCSPC based on CMOS single photon avalanche diode (SPAD) sensors exhibit unparalleled levels of miniaturization and portability, low fabrication costs, and high overall performance.[4] CMOS SPAD technology enables massively parallelized counting and timing of single photons in imaging, line and single point sensor formats. The per-pixel time-resolution offered by SPAD line sensors opens up new applications in hyperspectral scanning systems in microscopy, endoscopy as well as new modalities in FRET, fluorescence lifetime and Raman spectroscopies.[1,5,6,7]

A major drawback of TCSPC systems is the need to readout time-stamp information for each detected photon requiring a high output data rate which limits the maximum operating frequency.[5] Time-gated measurement can be used to lower data rates through detecting photons in two or more time-windows to extract fluorescence life-times. Several architectures have been proposed to address such challenges from 4 gated counters[5], per-pixel time to digital converters (TDCs)[6], time-gated memories[7], in-pixel center-of-mass computation[1], and off-chip FPGA TDCs.[8]

In this work we exploit a recently developed 512 x 16 x 2 line sensor array for time-resolved fluorescence spectroscopy which supplements the generation of TCSPC time-codes with on-chip histogramming functionality for each pixel, greatly increasing sensor throughput.[9] We employ on-chip histogramming for the first time at a per-pixel level achieving up to two orders of increase in SPAD photon processing rates enabling fast scanning or low I/O power time-resolved spectroscopic imaging. As a result we are able to acquire time-resolved spectral data at very high rates. We demonstrate the use of the sensor for time-resolved fluorescence, photobleaching and FRET experiments.

2. MATERIALS AND METHODS

2.1 Optical setup

The experimental setup is shown in Fig. 1. An epifluorescence setup collects fluorescence from a cuvette filled with varying Fluorescein amidite (FAM)/Tetramethylrhodamine(TAMRA) mixtures or from samples of purified Enhanced Green fluorescent protein/Red Fluorescent Protein (EGFP/RFP) affixed to microscope slides. The fluorescence is focused into a multimode fiber and relayed to a spectrograph consisting of dispersive optics with CMOS SPAD line sensor placed in focus.

The sample was illuminated by a Hamamatsu PLP10 483 nm pulsed laser diode at 50 MHz repetition rate. Peak power of the 483 nm pulsed laser was 349 mW, and the pulse length was 60 ps resulting in a 0.42 mW average output. Illumination on the specimen was 0.27 mW. For alignment and spectrograph resolutions tests a WhiteLaseMicro supercontinuum (NKT Photonics-Fianium, UK) was used. Dichroic filters (FF414-DI01-25X36, Semrock, USA, and custom three color design from Chroma, USA) were used to separate illumination from fluorescence. Spectrograph diffraction was accomplished using a volume phase holographic grating (1200 lp/mm at 600nm, Wasatch Photonics) with collimating and focusing lens optimized for efficiency and spectral resolution. To cover the 100 nm wavelength span across the 512 pixels of the line sensor the collimating lens used was a 50 mm focal length achromat (AC254-050-A-ML, Thorlabs, UK), while the focusing lens was 75 mm focal length achromat (AC508-075-A-ML).

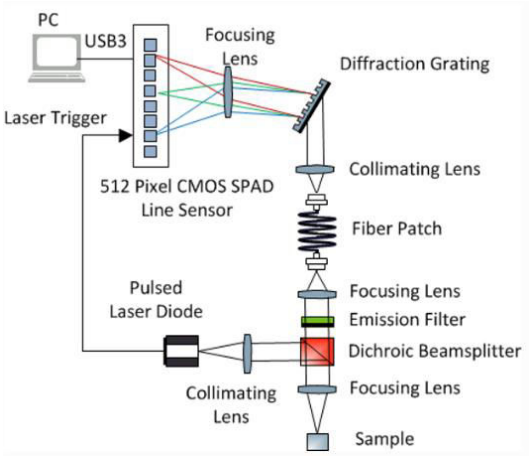

Figure 1. Experimental setup

2.2 CMOS SPAD line sensor

The sensor is a 1024 × 8 single photon avalanche diode (SPAD) based line sensor implemented in 0.13 µm CMOS technology with 23.78 µm pixel pitch at 49.31% fill factor. The sensor can operate in single photon counting (SPC) mode, time-correlated single photon counting (TCSPC) mode, or on-chip histogramming mode.

A simplified block diagram of the sensor is shown in Fig. 2 (a). The sensor consists of 512 pixels, 64 serialisers for reading out sensor data through 64 serial input/output PADs, one delay generator and some glue logic. As shown in Fig. 2 (b), each pixel has 32 SPADs (16 optimized for 450nm to 550nm and 16 optimized for 600nm to 900nm) which are arranged in an 8 rows × 2 columns format to double the spectral resolution. In addition, each pixel has some SPAD interface logic (e.g. SPAD quenching, pulse shortening, and pulse combiner), 5 clock trees (one for TDCs for providing a time reference for generating timestamps and the remaining 4 for generating 2 time gates), a 16-bit, 50ps time-to-digital converter (TDC), and a 32-bin histogram memory block which can be programmed to provide histogram window time ranges from 1.6ns to 204.8ns (i.e. from 50ps/bin to 6.4ns/bin zoomable time resolution).

Each histogram bin is implemented as a 10-bit ripple counter. For increased dynamic range two consecutive bins can be chained, halving the histogram bins to 16 while doubling the bin width to 20-bit. Bin widths can also be configured from 1 to 128 time-events per bin under the control of a histogram decoder. Together with a 50 ps resolution on-chip delay generator, this feature allows positioning and zooming of the histogram window to the spectral peak.

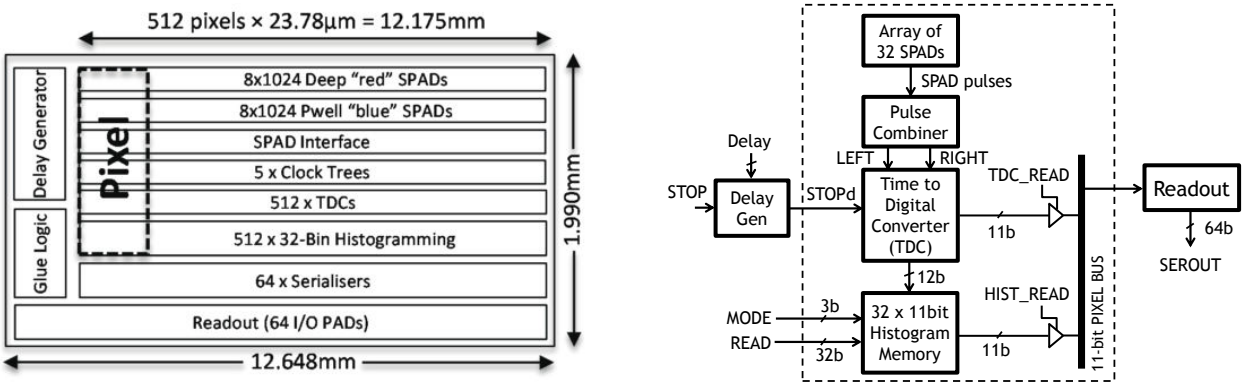

(a) (b)

Figure 2. (a) Line sensor block diagram, (b) Pixel block diagram

2.3 Sample Preparation

Stock solutions of FAM and TAMRA (Sigma Aldrich) were prepared at a concentration of 1 mM in phosphate buffered saline (PBS) to remove the effects of pH from measurements. To increase the viscosity of the samples, reduce evaporation and help bring fluorophores closer together the stock TAMRA solution was diluted 50% with glycerol (Sigma Aldrich). From these solutions, cuvettes of 2 ml mixtures of FAM/TAMRA were prepared along with reference concentrations of each dye by serial dilution whilst maintaining a solvent ratio of 50% PBS to 50% Glycerol. To maximise the observation of FRET, a donor (FAM) concentration of 50 µM was chosen and the acceptor (TAMRA) concentration was varied from 125 µM to 500 µM.

The addition of Glycerol has the added effect of lengthening the lifetime of the acceptor TAMRA. To show a greater difference in lifetime between donor and acceptor, solutions of FAM/TAMRA were produced in PBS only at a mix concentration of 10 µM FAM to 100 µM TAMRA along with corresponding reference solutions of just FAM and TAMRA in PBS.

To study FRET between EGFP and RFP purified samples of EGFP and RFP-EGFP complex FRET standards were prepared in PBS. A 2 µL aliquot of each sample was placed onto a microscope slide and the measurement performed immediately to avoid the sample drying.

2.4 FRET

Förster resonance energy transfer (FRET) is a non-radiative electro dynamical phenomenon in which excited state energy is transferred from one dye molecule (donor) to a different dye molecule (acceptor) without emission.[10] Donor-to-acceptor energy transfer leads to a reduction in donor fluorescence intensity and excited state lifetime accompanied by an increase in acceptor emission (sensitized emission). FRET depends on close proximity (1-10nm) between the donor and

acceptor molecules. The fluorescence quantum yield of the donor in absence of acceptor, refractive index of the solution, dipole angular orientation of each molecule and spectral overlap integral of the donor emission and acceptor absorption also influence the rate of energy transfer.

FRET efficiency, defined as the fraction of photons absorbed by the donor that is transferred to the acceptor, can be expressed in terms of experimentally measured lifetimes as

$$E = 1 - \frac{\tau_{DA}}{\tau_D} \tag{1}$$

where τ_{DA} is the lifetime of the donor in presence of an acceptor and τ_D is the lifetime of the donor in the absence of an acceptor. FRET efficiency can also be expressed as:

$$E = 1 - \frac{F_{DA}}{F_D} \tag{2}$$

where F_{DA} and F_D are the donor fluorescence intensities with and without an acceptor, respectively. When performing FRET measurements in solution care has to be taken to distinguish between other competing processes within the solution such as re-absorption of photons emitted by the donor in the acceptor's absorption region. Reabsorption occurs over the entire detection path length but does not affect the donor lifetime as the normal emission path is maintained. Therefore, fluorescence lifetime is superior to intensity measurements (the other most common method) for solution phase FRET measurements.

3. RESULTS AND DISCUSSION

Saha et al have previously reported FRET interactions in solution between Fluorescein and Rhodamine 6G[2] and Shah have investigated Uranin and Rhodamine 101 FRET pairs.[11] In this work we used FAM donor and TAMRA acceptor as a FRET pair. The emission spectrum of FAM has a very large overlap with the absorption of TAMRA in the region of 480nm - 600nm. This makes the dye pair ideal for FRET as there is a high degree of overlap in the molecular energy levels.

FAM, like most fluorescein derivatives is particularly prone to photo-bleaching. The photo-bleaching of FAM over a 20s laser exposure period is shown in Fig. 4. 600 successive spectra were obtained at time intervals of 30ms with 10ms exposure time per spectra. The sample was illuminated with a 50 MHz laser repetition rate and 483 nm laser source. This highlights our capability to measure full spectral lifetime data at a very rapid rate. It can be seen that there is a significant drop in intensity over this time period and therefore care must be taken when using intensities in ratiometric determination of processes such as FRET. This further highlights the advantages of lifetime based FRET determination as this is unaffected by bleaching.

In Fig. 5, we present time-resolved fluorescence spectra and their corresponding lifetime results for three distinct solutions: 50 μM FAM, 250 μM TAMRA, and a 50 μM FAM/250 μM TAMRA mix. Samples were illuminated with a 50MHz repetition rate and 483nm excitation laser source. Time-resolved spectra were obtained using on-chip histogramming with 1s exposure time and setting the histogram window to 0 – 25.6ns range. Fluorescence lifetimes were estimated based on mono-exponential fits using 16 histogram bin counts per pixel. As shown in Fig. 5 (h), TAMRA results are dominated by noise in the sub-560nm region since this corresponds to a region outside the fluorescence emission range. The mean lifetime of FAM (donor) is 3.3ns over the 507nm to 596nm wavelength range (see Fig. 5 (g)). The mean lifetime of TAMRA (acceptor) is 2.7ns above 560nm (see Fig. 5 (h)). The mean FAM/TAMRA mix lifetime is approximately 2.9ns below 540nm and remains at 3ns above 560nm (see Fig. 5 (i)).

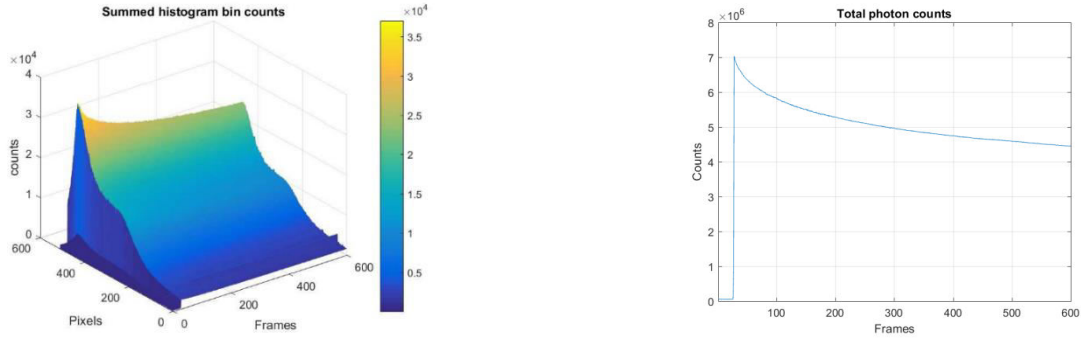

(a) (b)

Figure 4. Photobleaching of FAM. 600 successive frames at intervals of 30ms and 10ms exposure time per frame. (a) Photon counts per pixel, (b) Total photon counts of the pixel array.

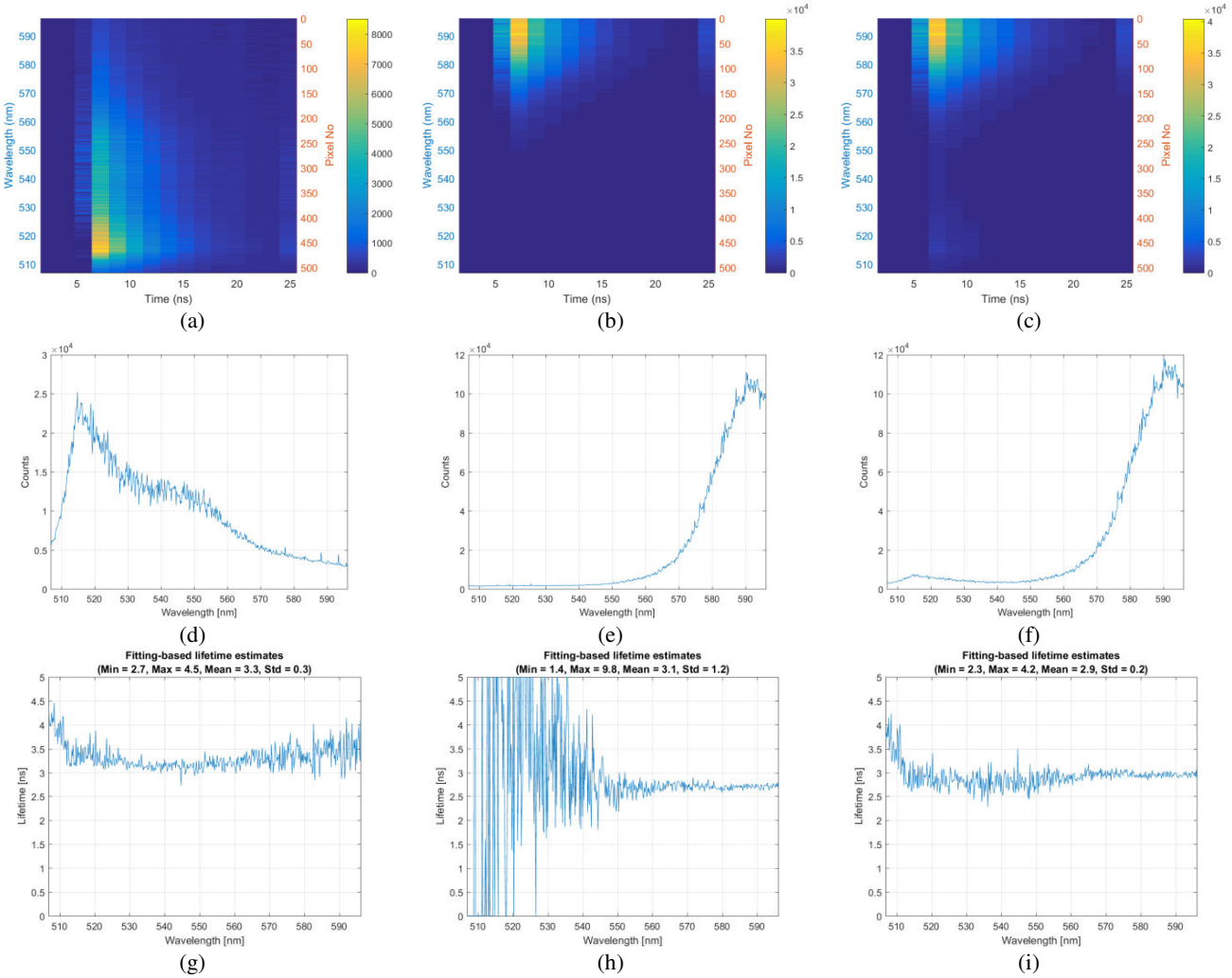

(a) (b) (c)

(d) (e) (f)

(g) (h) (i)

Figure 5. Time-resolved fluorescence spectrum, summed histogram bin counts and corresponding curve fitting based lifetime estimates of 50uM FAM (a, d, g), 250uM TAMRA (b, e, h), and 50uM FAM + 250uM TAMRA mixture (c, f, i), excited with a 50MHz repetition rate, 483nm laser source for a 1s exposure time.

Fig. 6 (a) shows estimated lifetimes of donor only (F50μM) and donor/acceptor mixture solutions where donor concentration was fixed at 50 μM and acceptor concentration varied from 125 μM to 500 μM in steps of 125 μM. There is clear decrease in spectral lifetimes of the donor/acceptor mixtures compared to donor and the amount of decrease is correlated to the donor/mixture concentration. For each donor/acceptor concentration, FRET efficiency was measured spectrally in the acceptor free region of 510nm to 540nm wavelength range using Eq. (1). As shown in Fig. 6 (b), the measured FRET efficiency varies with donor/acceptor concentration. The highest FRET efficiency is achieved with 500μM acceptor concentration, having an average efficiency of 20%. Similar results are obtained for 250 μM and 375 μM acceptor concentrations with average of 12% and 11% FRET efficiencies respectively. Finally, for the 50μM/125μM donor/acceptor mixture, it has the lowest FRET efficiency with an average of 5%.

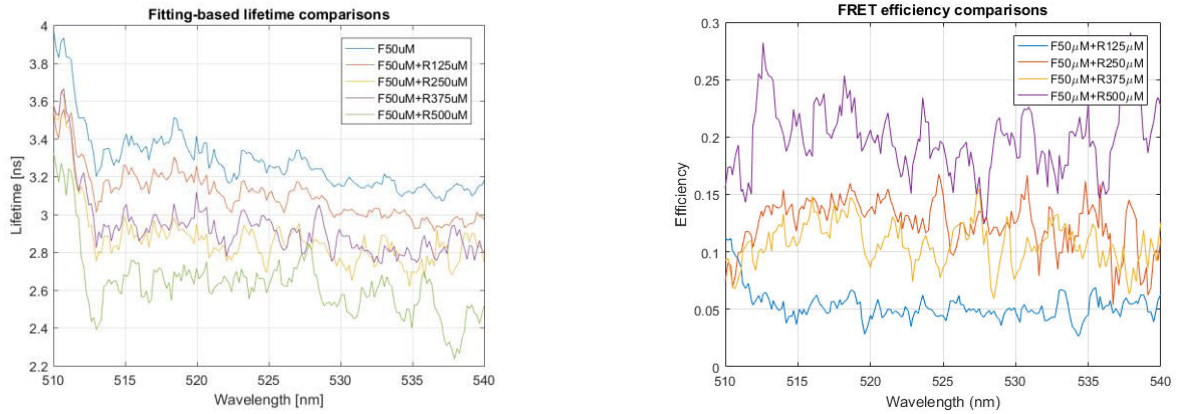

(a) (b)

Figure 6. (a) Spectral lifetime comparisons of donor and different donor/acceptor mixture solutions over the acceptor-free region of 510nm-540nm wavelength range. (b) FRET efficiency of each donor/acceptor mixture solution calculated with Eq. (1). A five-point moving average is used to smooth the data.

A direct comparison between acceptor concentration and FRET efficiency is shown in Fig. 7.

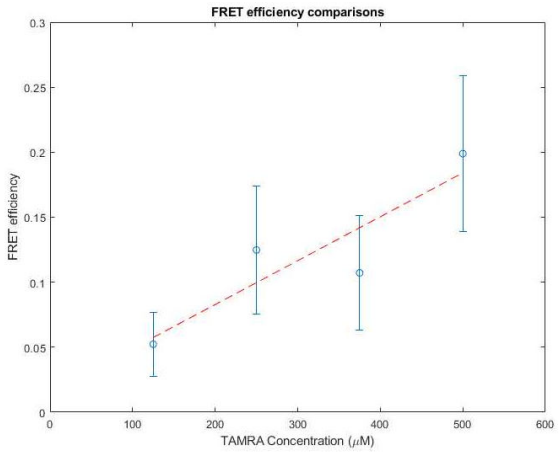

Figure 7. Comparison of FRET efficiency vs acceptor (TAMRA) concentration at a fixed donor (FAM) concentration of 50 μM.

In Fig. 8, we present lifetime results for three distinct solutions: 5μM FAM, 50 μM TAMRA, and 5 μM FAM/50 μM TAMRA mix in PBS only across the wavelength range (Fig. 8 (a)) along with change in lifetime across the donor region (Fig. 8 (b)) showing a FRET efficiency of ~5%. Samples were measured using the same experimental settings as previously. Fluorescence lifetimes were estimated based on mono-exponential fits using 16 histogram bin counts per pixel. Without the presence of Glycerol the lifetime of TAMRA is greatly reduced, thus making observation of changes in both donor and acceptor lifetime clearly visible.

From Fig. 8 the reduction in lifetime of the donor is clearly observed along with an apparent increase in acceptor lifetime. This would be consistent with energy transfer pumping emissive states in the acceptor. The ability to measure the whole spectral region of interest thus opens up new avenues of analysis for this type of system.

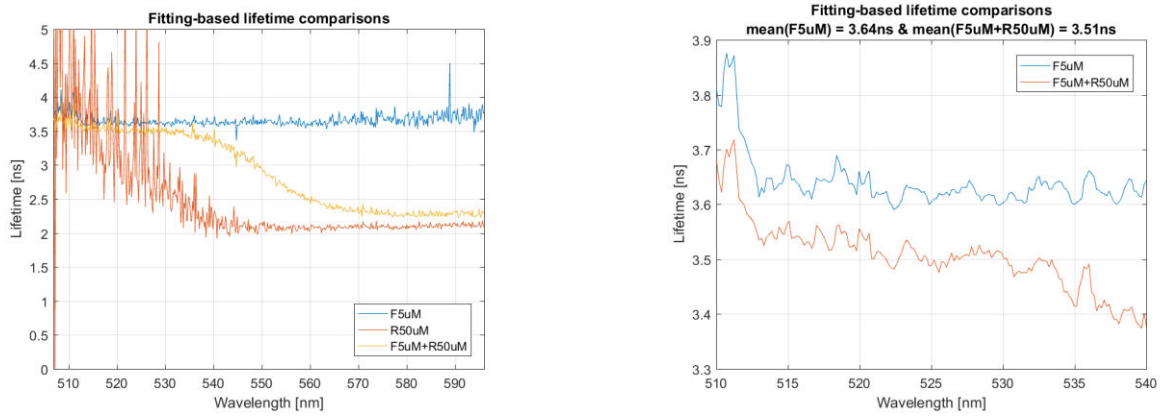

(a) (b)

Figure 8: (a) Spectral fitting-based lifetime comparisons of donor, acceptor, and donor/acceptor mixture of FAM/TAMRA recorded with 1s exposure, (b) Comparing lifetimes of donor and donor/acceptor mixture solutions over the acceptor-free region (i.e. 510nm-540nm) which shows an average of 0.13ns reduction in lifetime for donor/acceptor mixture compared to donor only solution.

In Fig. 9, we present time-resolved fluorescence spectra, summed histogram bin counts and corresponding curve fitting based lifetime estimates of EGFP and RFP-EGFP FRET standards. Measurements were performed using the same experimental settings as for FAM/TAMRA solution measurements. Fluorescence lifetimes were estimated based on mono-exponential fits using 16 histogram bin counts per pixel. There is a significant reduction in the number of photons captured for RFP-EGFP compared to EGFP sample alone. There is also clear reduction in spectral lifetimes across the wavelength range from 510nm to 590nm indicating significant FRET efficiency.

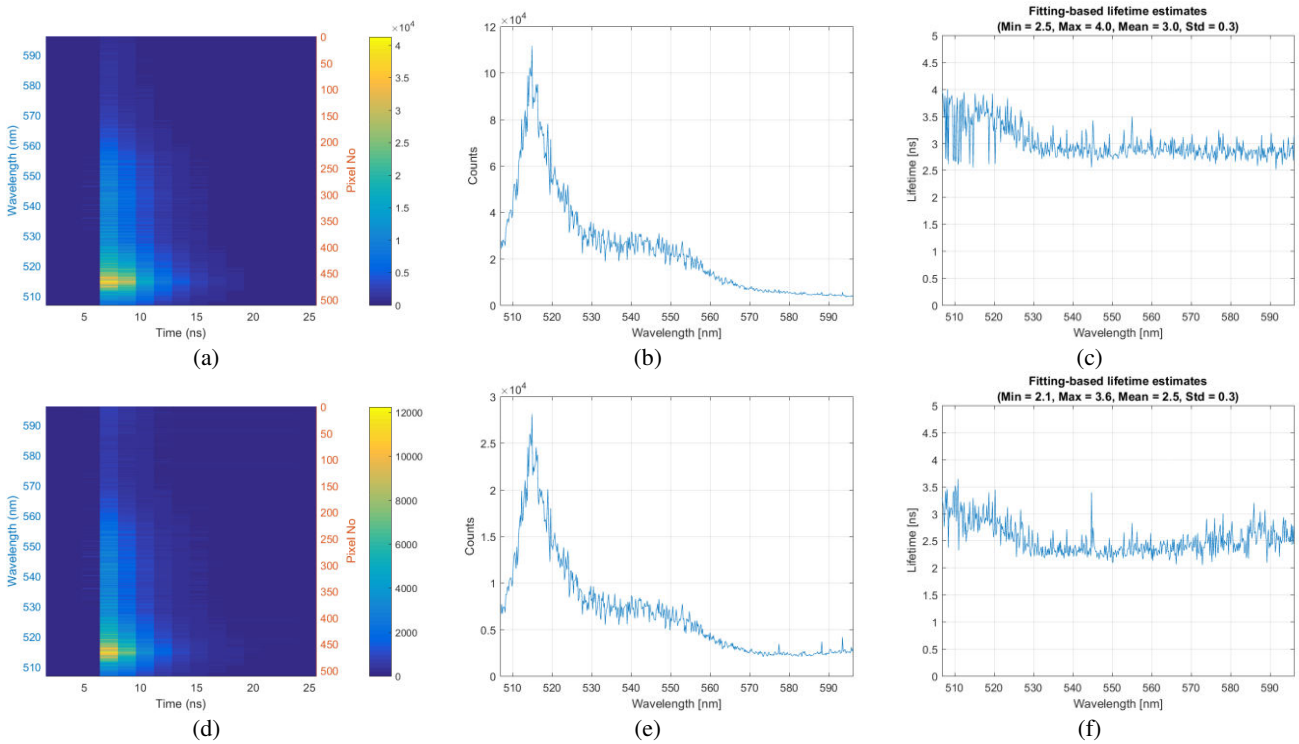

(a) (b) (c)

(d) (e) (f)

Figure 9. Time-resolved fluorescence spectrum, summed histogram bin counts and corresponding curve fitting based lifetime estimates of EGFP (a, b, c) and RFP-EGFP FRET standards (d, e, f), excited with a 50MHz repetition rate and 483nm laser source.

FRET efficiency was calculated for the wavelength range of 510nm-540nm. As shown in Fig. 10 (a), EGFP and RFP-EGFP FRET standards have an average lifetime of 3.19ns and 2.63ns respectively. The corresponding FRET efficiencies calculated based on Eq. (1) are shown in Fig. 10 (b), showing an average of 17% efficiency.

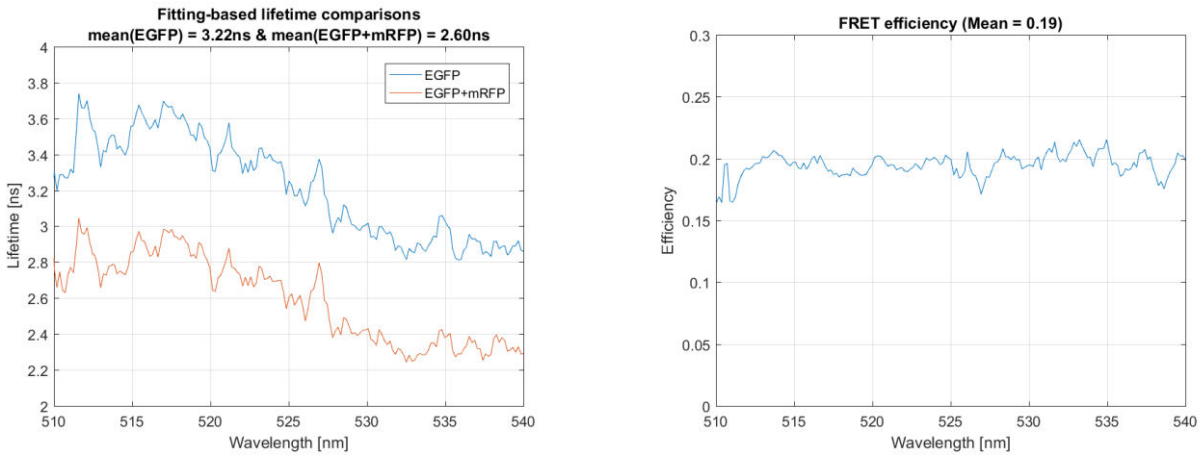

(a) (b)

Figure 10. (a) Spectral lifetime comparisons of EGFP and RFP-EGFP FRET standards over the 510nm-540nm wavelength range. (b) Spectral FRET efficiency calculated with Eq. (1).

4. CONCLUSIONS

We have demonstrated the use of an advanced CMOS SPAD array sensor with on-chip histogramming ability to resolve the lifetime information essential for the determination of FRET efficiency at extremely high rates. The ability to measure lifetime over the complete donor-acceptor region in a single shot, enabled by on-chip histogramming, gives an unprecedented amount of information regarding the inter-molecular processes involved. In particular in simple molecular solutions, a system where traditionally it has been extremely difficult to observe processes such as FRET, we demonstrate that the collection of complete spectral and lifetime data provides the required information to extract the FRET process from other competing mechanisms such as re-absorption events which affect intensity but not lifetime. Further, by observing the entire spectrum in a single shot, effects on the donor and acceptor emission properties can be studied simultaneously. The use of a known FRET pair, GFP-RFP validates this system for use in this extremely important field. Finally, as highlighted throughout the speed at which these measurements were taken is key in unlocking new areas of research in FRET imaging and analysis. We have demonstrated the ability to measure full spectral lifetime data, from solutions, on the millisecond timescale, fast enough to measure dynamic processes.

ACKNOWLEDGEMENTS

This research was funded by the Engineering and Physical Science Research Council (EPSRC, United Kingdom) Interdisciplinary Research Collaboration (grant number EP/K03197X/1) (Proteus), the Richard Dimbleby Cancer Research Trust and Leverhulme Trust project RPG-2015-105. We would also like to thank EPSRC and MRC Centre for Doctoral Training in Optical Medical Imaging, OPTIMA, (grant number EP/L016559/1). The authors are most grateful to Dr. Simon Ameer-Beg for his support. We would also like to thank ST Microelectronics, Imaging Division, Edinburgh, for their support in manufacturing the CMOS SPAD line array.

REFERENCES

[1] Krstajić, N., Levitt, J., Poland, S., Ameer-Beg, S. and Henderson, R., "256 × 2 SPAD line sensor for time resolved fluorescence spectroscopy," Opt. Express 23(5), 5653 (2015).

[2] Saha, J., Datta Roy, A., Dey, D., Chakraborty, S., Bhattacharjee, D., Paul, P. K. and Hussain, S. A., "Investigation of Fluorescence Resonance Energy Transfer between Fluorescein and Rhodamine 6G," Spectrochim. Acta Part A Mol. Biomol. Spectrosc. 149, 143–149 (2015).

[3] Becker, W., [Advanced Time-Correlated Single Photon Counting Applications], Springer International Publishing, Cham (2015).

[4] Palubiak, D. P. and Deen, M. J., "CMOS SPADs: Design Issues and Research Challenges for Detectors, Circuits, and Arrays," IEEE J. Sel. Top. Quantum Electron. 20(6), 409–426 (2014).

[5] Pancheri, L. and Stoppa, D., "A SPAD-based pixel linear array for high-speed time-gated fluorescence lifetime imaging," 2009 Proc. ESSCIRC, 428–431, IEEE (2009).

[6] Nissinen, I., Nissinen, J., Holma, J. and Kostamovaara, J., "A 4×128 SPAD array with a 78-ps 512-channel TDC for time-gated pulsed Raman spectroscopy," Analog Integr. Circuits Signal Process. 84(3), 353–362 (2015).

[7] Maruyama, Y., Blacksberg, J. and Charbon, E., "A 1024×8, 700-ps Time-Gated SPAD Line Sensor for Planetary Surface Exploration With Laser Raman Spectroscopy and LIBS," IEEE J. Solid-State Circuits 49(1), 179–189 (2014).

[8] Burri, S., Homulle, H., Bruschini, C. and Charbon, E., "LinoSPAD: a time-resolved 256×1 CMOS SPAD line sensor system featuring 64 FPGA-based TDC channels running at up to 8.5 giga-events per second," Proc. SPIE 9899, 98990D (2016).

[9] Erdogan, A. T., Walker, R., Finlayson, N., Krstajic, N., Williams, G. O. S. and Henderson, R. K., "A 16.5 giga events/s 1024 × 8 SPAD line sensor with per-pixel zoomable 50ps-6.4ns/bin histogramming TDC," 2017 Symp. VLSI Circuits, C292–C293, IEEE (2017).

[10] Biskup, C., Zimmer, T., Kelbauskas, L., Hoffmann, B., Becker, W., Bergmann, A. and Benndorf, K., "Multi-Dimensional Fluorescence Lifetime and FRET Measurements," Microsc. Res. Tech. 70(2007), 442–451 (2007).

[11] Shah, S., Gryczynski, Z., Chib, R., Fudala, R., Baxi, A., Borejdo, J., Synak, A. and Gryczynski, I., "Demonstration of FRET in solutions," Methods Appl. Fluoresc. 4(1), 15001 (2016).